Acta Cryst. (1975). B31, 76

The Crystal Structure of P^1, P^2-Di-β-naphthyl Pyrophosphate Dicyclohexylammonium Salt

BY M. K. WOOD, M. SAX AND J. PLETCHER

Biocrystallography Laboratory, Veterans Administration Hospital, Pittsburgh, Pa. 15240, *U.S.A. and Department of Crystallography, University of Pittsburgh, Pittsburgh, Pa.* 15260, *U.S.A.*

(*Received* 20 *March* 1974; *accepted* 19 *July* 1974)

The crystal structure of P^1,P^2-di-β-naphthyl pyrophosphate dicyclohexylammonium salt $\{(C_{20}H_{14}O_7P_2)^{2-} 2(C_6H_{14}N)^+\}$ is the first reported determination of a pyrophosphate diester. The molecule is extended and the pyrophosphate moiety is in the staggered conformation. The torsion angles with respect to bridging oxygens sequentially along the P–O bonds are $-ap$, sc, ac, and sc. An unusually small torsion angle with respect to a phosphoryl oxygen is only 3·2°. The O–P–O valence angles and the O···O distances within the pyrophosphate tetrahedra deviate more than expected from the values predicted by Baur's correlations. These discrepancies can be attributed to non-bonded interactions between phosphate oxygens and substituent atoms. We propose that O–P–O valence angles are significantly decreased relative to their predicted values if the oxygens are *anti* to a substituent on the phosphate and are increased if they are *syn*. An unusual aspect of the hydrogen bonding is the coplanarity of the P, O and N atoms in a quaternary complex. Crystals of DNPP are monoclinic, space group $P2_1/c$, with four molecules in the unit cell of dimensions $a = 13{\cdot}285$ (3), $b = 30{\cdot}259$ (7), $c = 8{\cdot}217$ (2) Å and $\beta = 109{\cdot}37$ (3)°. The diffractometer intensity data were obtained with graphite-monochromated Cu $K\alpha$ radiation. Except for the pyrophosphate oxygens, the asymmetric unit has an approximate center of symmetry. The pseudocenter is at $\frac{1}{4}\frac{1}{2}\frac{1}{2}$, resulting in a subcell such that the average intensity of reflections with an even h index is four times that of their odd counterparts. The subcell data only were used in the direct solution of the structure. Refinement of the full structure required the use of a weighting scheme which did not discriminate against the systematically weak data subset. The structure was refined by full-matrix least-squares techniques to a conventional R value of 0·065 for the 3418 observed reflections.

Introduction

This determination of the crystal structure of the title compound (DNPP) is the first to be carried out on a pyrophosphate diester at atomic resolution. One of the specific aims of this study is to distinguish the effective interactions which influence pyrophosphate diester conformation. The diester pyrophosphate linkage is essential for the activity of many naturally occurring substances (*e.g.*, uridine-5′-diphosphoglucose (UDPG), nicotinamide adenine dinucleotide (NAD), coenzyme A) which have thus far resisted crystallization. As activity of these cofactors does not appear to depend upon metal–ion ligation by the pyrophosphate, and as enzyme binding may involve hydrogen bonding between amino groups on the protein and the pyrophosphate, this structure is a model for some aspects of the conformation of physiologically active pyrophosphate diesters. NAD has been observed in complex with an enzyme in the studies of lactate dehydrogenase (LDH). There, the best fit to the electron density is achieved by placing the pyrophosphate in the staggered conformation and the diribotide pyrophosphate in an extended conformation (Adams, McPherson, Rossmann, Shevitz & Wanacott, 1970).

Experimental

From a sample provided by Professor F. Cramer, Max Planck Institute, Göttingen, Germany, 0·01 g was dissolved in a hot solvent composed of dimethyl sulfoxide (1 ml), ethanol (1 ml) and pyridine (1 ml). This solution was slowly concentrated by evaporation at elevated temperature for several weeks, but it was not taken to dryness. Crystals grew as clear, colorless plates, most of which were twinned. Although they were of poor quality, a useable single crystal having dimensions $0{\cdot}3 \times 0{\cdot}1 \times 0{\cdot}2$ mm was cut from a larger specimen. An oscillation photograph which showed alternate rows of weak spots revealed the presence of a subcell. The space group, deduced as $P2_1/c$ from Weissenberg photographs, was confirmed later in the structure determination. The crystal data are given in Table 1. The lattice constants were determined by a least-squares fit of the orientation and 2θ angles for 12 reflections (Picker, 1972) measured with Cu $K\alpha$ radiation on a diffractometer. The 2θ values ranged between 28 and 56°. The intensity data were collected with graphite monochromated Cu $K\alpha$ radiation on a Picker FACS-1 X-ray diffractometer. 5111 independent reflections were measured to a maximum 2θ value of 127·00° ($d_{min} = 0{\cdot}8607$ Å) by the $\theta{:}2\theta$ scan technique. The background was counted for 20 s at each end of the scan range. Because of the importance of the structure and the difficulty of the crystallization, data were collected on a crystal that would not ordinarily have been considered of adequate quality for diffractometry. An examination of several peaks by ω-scans under fine conditions on the diffractometer revealed that their shapes were not Gaussian, and diffraction could be observed as far as

2° from the centroid. Data collection conditions were adjusted to measure as much of the diffracted intensity from each peak as possible. The conditions used were 4° take-off angle with the symmetrically variable apertures fully open and a minimum 2θ scan width of 3·00°. In this way good reproducibility was achieved among equivalent quadrants, although the background was high.

Table 1. *Crystal data at* 24°C

P^1,P^2-Di-β-naphthyl pyrophosphate dicyclohexylammonium salt

$(C_{20}H_{14}O_7P_2)^{2-}$, $2(C_6H_{14}N)^+$	M.W. 628·65
$a=13{\cdot}285$ (3) Å	$D_x=1{\cdot}340$ g cm^{-3}
$b=30{\cdot}259$ (7)	m.p. 248°C
$c=8{\cdot}217$ (2)	
$\beta=109{\cdot}37$ (3)°	
$V=3116$ Å^3	$Z=4$
μ(Cu $K\alpha$) = 16·8 cm^{-1}	$F(000)=1336$

Space group: $P2_1/c$ from systematic absences $h0l$ for $l=2n+1$, $0k0$ for $k=2n+1$.

The weak reflections exhibited a high incidence of systematic error. Three standard reflections, monitored after every 50 reflections, showed an overall decay of less than 5%. No correction was made.

The intensity data were converted to relative structure factor amplitudes after correction for Lorentz and polarization effects appropriate for graphite-monochromated ($2\theta_m=26{\cdot}16°$) radiation (Picker Corporation, 1972). Of the independent reflections, 1693 (33·1%) were unobserved, as defined by $|F|\leq 6\sigma(F)$ where $|F|$ is the structure amplitude and where $\sigma(F)$ is given by $(1/2\mathrm{Lp}|F|)\sigma(I)$; Lp is the Lorentz–polarization factor, $\sigma(I)=[I_t+k^2B]^{1/2}$, $I=I_t-B_t$, $B_t=kB$, $B=(b_1+b_2)$, $k=t_s/2t_b$, $I_t=(10S+5)$, $b_1=(10C_1+5)$, $b_2=(10C_2+5)$, $S=$the number of decacounts accumulated during the scan requiring time t_s, and C_1 and C_2 are the background decacounts accumulated in time t_b at either end of the scan range.

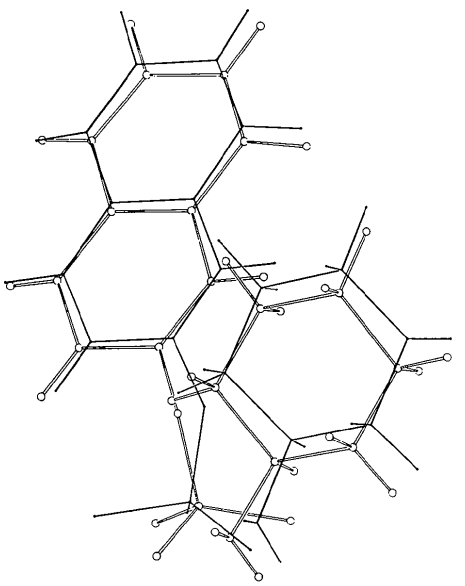

Fig. 1. A superposition of half of the asymmetric unit on the other half inverted through the pseudocenter of symmetry at $\frac{1}{4}\frac{1}{2}\frac{1}{2}$ as drawn by the *ORTEP* program (Johnson, 1965).

Solution of the structure

The structure was solved with the program *MULTAN* (Germain, Main & Woolfson, 1971). The normalized structure factor amplitudes, $|E|$, were derived using the overall thermal parameter and the scale factor found by the method of Wilson. There is extreme rational dependence in the indices; the $\langle E^2(h_ok l)\rangle:\langle E^2(h_ek l)\rangle$ ratio is 0·24, where o and e refer to odd and even values of h respectively. The difficulty in accurately measuring weak reflections gave us some concern that we had the correct space group.

The initial attempts at *MULTAN* solutions were carried out on E's that had been renormalized so that $\langle E^2(h_ek l)\rangle\approx\langle E^2(h_ok l)\rangle\approx 1{\cdot}0$. A number of possible solutions were obtained for the space groups $P2_1$, $P2_1/m$, $P2_1/c$ and $P2_1/a$. Only the E map calculated for the best solution from $P2_1/c$ gave a possible phosphorus position consistent with the Patterson function; no other details of the structure could be detected. At this point we attempted a solution using the subcell data only.

Accordingly, the $E(h_ok l)$ were ignored and $E(h_e/2, k, l)$ only were used, that is, the h index of reflections having $h=2n$ was halved prior to the solution. An E map calculated from the best *MULTAN* solution for $P2_1/c$ revealed the structure. The subcell condition, therefore, is confirmed to be a pseudocenter of symmetry at $\frac{1}{4}\frac{1}{2}\frac{1}{2}$ in the true cell and corresponds to a halving of the cell along the a axis. The phosphoryl oxygens of the pyrophosphate do not obey the subcell condition and appeared at approximately half-weight. Fig. 1 shows the superposition of the final coordinates of the two halves of the asymmetric unit using the pseudocenter of symmetry.

Refinement

The subcell structure was refined by the full-matrix least-squares method to a conventional R value of 0·22, with the half-cell data only. The function $\sum w(k|F_o|-|F_c|)^2$ was minimized (Shiono, 1971). Initially, weights w were set equal to $[\sigma(F)]^{-2}$. The subcell constraint was broken by ordering the pyrophosphate oxygens in a chemically sensible manner, by allowing the atoms previously assumed to be centrosymmetrically related to move independently and by refining on the full data set. Several cycles of refinement failed to converge, indicating that a different weighting scheme might be needed. Examining $\langle w(F_o-F_c)^2\rangle$ as a function of $|F|$ and, more importantly of the Miller indices showed that the $h_ok l$ and the weak reflections in general

were not properly contributing to the refinement process. Therefore, the weights were modified to give a value of unity to $\langle w(F_o-F_c)^2\rangle$ as a function of $|F|$ using three line segments derived from a plot of $\langle(|F_o|-|F_c|)^2\rangle$ *vs.* $|F|$. Convergence was then rapid.

The weights were revised by this procedure throughout the remainder of this refinement, as the model was improved. The final weighting function was for $|F| \le 36$: $w = 1{\cdot}9$, for $36 < |F| \le 78$: $w = -0{\cdot}2 + 0{\cdot}057\,|F|$ and for $78 < |F|$: $w = 1{\cdot}9 + 0{\cdot}031\,|F|$. This 'tailoring' of the weighting scheme was felt to be essential in order to insure that the relatively weaker h_okl reflections, which are the only ones affected by the deviation of the structure from the pseudocenter, had an appropriate influence on the structure refinement. A discussion of the importance of weighting in refining the 'difference' structure with respect to the 'mean' structure is given by Rae (1973); other effects of weighting are discussed by Dunitz & Seiler (1972) and Cruickshank (1970). Anisotropic thermal parameters were introduced and subsequently hydrogens were found by difference Fourier synthesis. Refining all positional parameters, the anisotropic thermal parameters of the heavy atoms and the isotropic thermal parameters of the hydrogen atoms brought convergence at a conventional R value of 0·064 for the 3418 observed reflections. The unobserved reflections were not included in the refinement.

An additional cycle of refinement was carried out including the 16% of the unobserved reflections that calculated as observed F's; this resulted in no significant effect on the parameters. A procedure similar to this has been discussed by Dunning & Vand (1969). The R value for all reflections is 0·072. The scattering

Table 2. *Positional and thermal parameters*

Positions are designated in fractional coordinates of unit-cell axes; estimated standard deviations in parentheses.

(*a*) Nonhydrogen atoms. Positional parameters $\times 10^4$, thermal parameters $Å^2 \times 10^3$. Thermal parameters defined as $\exp\{-2\pi^2(U_{11}h^2a^{*2}+\cdots+2U_{12}hka^*b^*+\cdots)\}$.

	x	y	z	U_{11}	U_{22}	U_{33}	U_{12}	U_{13}	U_{23}
P(1)	1731 (0·8)	4735 (0·4)	3608 (1·4)	17 (0·5)	36 (0·5)	28 (0·6)	0 (0·4)	8 (0·4)	0 (0·5)
P(2)	3151 (0·8)	5273 (0·4)	6440 (1·5)	17 (0·5)	38 (0·5)	29 (0·6)	0 (0·4)	11 (0·4)	−1 (0·5)
O(1)	2330 (3)	4295 (1)	4546 (4)	52 (2)	45 (2)	39 (2)	15 (2)	28 (2)	6 (2)
O(2)	2187 (2)	4888 (1)	2272 (4)	26 (2)	49 (2)	34 (2)	0 (2)	14 (1)	7 (2)
O(3)	567 (2)	4666 (1)	3088 (5)	11 (1)	62 (2)	52 (2)	−9 (2)	6 (1)	0 (2)
O(4)	2050 (2)	5053 (1)	5245 (4)	16 (2)	54 (2)	41 (2)	−2 (1)	13 (1)	−12 (2)
O(5)	3154 (3)	5217 (1)	8229 (4)	28 (2)	57 (2)	30 (2)	0 (2)	10 (1)	3 (2)
O(6)	4055 (2)	5124 (1)	5919 (4)	15 (1)	56 (2)	45 (2)	4 (1)	18 (1)	0 (2)
O(7)	2962 (2)	5781 (1)	5885 (4)	29 (2)	41 (2)	53 (2)	0 (2)	31 (2)	0 (2)
N(1)	1229 (4)	153 (2)	3625 (6)	25 (2)	62 (3)	35 (3)	−1 (2)	11 (2)	−11 (2)
N(2)	4039 (3)	9729 (2)	6959 (6)	21 (2)	48 (3)	41 (3)	1 (2)	11 (2)	−6 (2)
C(1)	2422 (4)	3576 (2)	3464 (6)	28 (2)	46 (3)	34 (3)	4 (2)	10 (2)	6 (2)
C(2)	2807 (4)	3988 (2)	3755 (6)	31 (2)	38 (3)	32 (3)	9 (2)	11 (2)	2 (2)
C(3)	3759 (4)	4116 (2)	3439 (7)	27 (2)	45 (3)	45 (3)	1 (2)	14 (2)	5 (3)
C(4)	4265 (4)	3808 (2)	2771 (7)	27 (2)	59 (4)	48 (3)	3 (3)	15 (2)	5 (3)
C(5)	4372 (5)	3050 (2)	1652 (8)	45 (3)	68 (5)	60 (4)	22 (3)	21 (3)	−3 (3)
C(6)	3963 (6)	2635 (3)	1315 (9)	72 (5)	68 (5)	55 (4)	32 (4)	14 (3)	−9 (3)
C(7)	3027 (6)	2514 (2)	1673 (10)	68 (5)	42 (4)	75 (5)	7 (3)	4 (4)	−8 (3)
C(8)	2550 (5)	2815 (2)	2394 (7)	51 (4)	48 (3)	44 (3)	4 (3)	11 (3)	3 (3)
C(9)	2921 (4)	3248 (2)	2749 (7)	31 (3)	47 (3)	38 (3)	4 (2)	11 (2)	2 (2)
C(10)	3872 (4)	3377 (2)	2386 (7)	35 (3)	56 (4)	43 (3)	10 (3)	19 (2)	1 (3)
C(11)	2645 (4)	6502 (2)	6673 (6)	26 (2)	44 (3)	36 (3)	−2 (2)	10 (2)	5 (2)
C(12)	2329 (3)	6077 (2)	6439 (6)	23 (2)	42 (3)	38 (3)	3 (2)	13 (2)	4 (2)
C(13)	1358 (4)	5933 (2)	6641 (7)	25 (2)	37 (3)	47 (3)	0 (2)	15 (2)	2 (2)
C(14)	787 (4)	6233 (2)	7227 (7)	23 (2)	46 (3)	49 (3)	0 (2)	15 (2)	5 (3)
C(15)	539 (5)	6985 (2)	8237 (8)	40 (3)	56 (4)	55 (4)	13 (3)	16 (3)	−1 (3)
C(16)	879 (5)	7402 (2)	8596 (9)	66 (4)	51 (4)	64 (4)	14 (3)	24 (3)	−4 (3)
C(17)	1822 (6)	7546 (2)	8298 (9)	68 (4)	40 (3)	61 (4)	−1 (3)	11 (3)	−2 (3)
C(18)	2381 (5)	7257 (2)	7652 (8)	49 (3)	43 (3)	53 (3)	−4 (3)	20 (3)	4 (3)
C(19)	2064 (4)	6815 (2)	7281 (7)	28 (2)	41 (3)	39 (3)	−2 (2)	9 (2)	5 (2)
C(20)	1099 (4)	6669 (2)	7567 (7)	30 (2)	42 (3)	45 (3)	4 (2)	17 (2)	5 (2)
C(21)	980 (4)	608 (2)	2969 (7)	29 (3)	63 (4)	31 (3)	4 (3)	11 (2)	−5 (3)
C(22)	99 (5)	803 (2)	3563 (10)	27 (3)	71 (5)	77 (5)	2 (3)	22 (3)	−21 (4)
C(23)	−144 (5)	1275 (3)	2964 (10)	47 (4)	73 (5)	64 (4)	17 (3)	1 (3)	−11 (4)
C(24)	843 (6)	1563 (3)	3539 (10)	62 (4)	60 (5)	57 (4)	6 (3)	4 (3)	−5 (4)
C(25)	1719 (7)	1362 (3)	2919 (13)	67 (5)	75 (6)	90 (6)	−8 (4)	39 (4)	5 (5)
C(26)	1976 (4)	895 (2)	3560 (9)	27 (3)	68 (4)	61 (4)	−1 (3)	21 (3)	−8 (3)
C(27)	4139 (3)	9256 (2)	7407 (6)	18 (2)	52 (3)	28 (3)	1 (2)	7 (2)	−6 (2)
C(28)	5038 (4)	9050 (2)	6911 (8)	22 (3)	64 (4)	53 (4)	2 (3)	13 (3)	−14 (3)
C(29)	5149 (5)	8564 (2)	7327 (9)	35 (3)	58 (4)	67 (4)	9 (3)	9 (3)	−12 (3)
C(30)	4110 (5)	8316 (2)	6532 (10)	49 (4)	57 (4)	58 (4)	4 (3)	0 (3)	−10 (3)
C(31)	3208 (5)	8529 (2)	7029 (9)	43 (3)	64 (4)	62 (4)	−15 (3)	20 (3)	−2 (3)
C(32)	3086 (4)	9014 (2)	6577 (8)	21 (2)	57 (4)	57 (4)	−6 (3)	15 (2)	−9 (3)

factor tables of Cromer & Waber (1965) were used for P, O, N and C and that of Stewart, Davidson & Simpson (1965) for the hydrogen atoms. The final difference synthesis had no peaks greater than 0·3 e $Å^{-3}$. The final positional and thermal parameters of the atoms are listed in Table 2.*

Table 2 (*cont.*)

(*b*) Hydrogen atoms. Positional parametres $\times 10^3$; temperature factors $(Å^2) \times 10^3$.

	x	*y*	*z*	*U*
H(N1)	143 (3)	15 (1)	481 (6)	2 (1)
H′(N1)	64 (6)	0 (2)	312 (9)	8 (2)
H″(N1)	185 (9)	3 (3)	328 (13)	15 (4)
H(N2)	388 (4)	974 (2)	570 (7)	4 (1)
H′(N2)	458 (5)	989 (2)	743 (8)	5 (2)
H″(N2)	356 (7)	989 (3)	712 (11)	9 (3)
H(C1)	182 (5)	347 (2)	382 (7)	5 (2)
H(C3)	401 (4)	442 (2)	363 (7)	5 (2)
H(C4)	479 (5)	391 (2)	247 (8)	7 (2)
H(C5)	500 (6)	315 (2)	127 (9)	9 (2)
H(C6)	432 (4)	240 (2)	91 (7)	5 (2)
H(C7)	274 (5)	221 (2)	123 (7)	6 (2)
H(C8)	185 (5)	274 (2)	271 (8)	7 (2)
H(C11)	328 (4)	661 (2)	641 (7)	5 (1)
H(C13)	114 (4)	564 (2)	646 (6)	3 (1)
H(C14)	13 (5)	611 (2)	741 (8)	6 (2)
H(C15)	−4 (6)	686 (2)	851 (9)	9 (2)
H(C16)	55 (5)	764 (2)	908 (8)	6 (2)
H(C17)	206 (5)	784 (2)	870 (8)	6 (2)
H(C18)	308 (5)	734 (2)	730 (8)	7 (2)
H(C21)	70 (4)	60 (2)	165 (7)	4 (1)
H(C22)	41 (6)	82 (3)	481 (11)	10 (3)
H′(C22)	−54 (6)	65 (2)	306 (9)	9 (2)
H(C23)	−44 (4)	130 (2)	161 (8)	5 (2)
H′(C23)	−66 (5)	142 (2)	342 (8)	7 (2)
H(C24)	98 (5)	155 (2)	485 (8)	5 (2)
H′(C24)	66 (5)	188 (2)	309 (9)	8 (2)
H(C25)	229 (6)	154 (2)	333 (10)	8 (2)
H′(C25)	147 (6)	138 (2)	157 (11)	11 (3)
H(C26)	233 (5)	91 (2)	508 (9)	7 (2)
H′(C26)	243 (6)	75 (2)	328 (9)	7 (2)
H(C27)	433 (4)	927 (2)	869 (7)	4 (1)
H(C28)	481 (4)	909 (1)	575 (6)	2 (1)
H′(C28)	577 (5)	920 (2)	767 (8)	6 (2)
H(C29)	545 (5)	852 (2)	882 (8)	6 (2)
H′(C29)	567 (6)	845 (3)	697 (10)	8 (3)
H(C30)	397 (5)	835 (2)	536 (8)	5 (2)
H′(C30)	417 (5)	797 (2)	687 (8)	6 (2)
H(C31)	250 (6)	838 (2)	629 (10)	10 (2)
H′(C31)	341 (4)	852 (2)	827 (7)	3 (1)
H(C32)	280 (6)	905 (3)	526 (11)	11 (3)
H′(C32)	262 (5)	920 (2)	680 (8)	6 (2)

Discussion

The bond distances, valency angles and the numbering of the atoms are shown in Fig. 2. We have used half-normal probability plot analysis (Abrahams & Keve, 1971; Hamilton & Abrahams, 1972) to compare the pseudocentrosymmetrically related moieties of this structure. Results derived from data containing a random normal distribution of error would give a linear plot of zero intercept and unit slope. Since the pyrophosphate moiety does not follow the pseudosymmetry, it has been omitted. Fig. 3(*a*) shows the comparison of the bond distances and valency angles. A least-squares line through these points has a slope of 0·8 with some non-linearity at the extreme. Thus, the pseudosymmetrically related parameters agree better than would be predicted on the basis of the e.s.d.'s. A possible explanation lies in the subcell characteristic of the structure. Both systematic and random errors in the subcell data ($h_e kl$) and defects in the least-squares model will affect the independent moieties almost equally, perhaps giving rise to this 'abnormally' good agreement. A less likely alternative is that the e.s.d.'s in the positional parameters are overestimated. Fig. 3(*b*) shows the comparison of thermal parameters. The slope of the least-squares line is 1·6, although the plot is linear. One interpretation of this plot is that there are differences in the thermal parameters of the pseudocentrosymmetrically related moieties due to actual differences in their environments. However, a more likely explanation may be that the e.s.d.'s in the thermal parameters have been underestimated.

Phosphate dimensions

Baur (1974) had used a phenomenological approach to develop a treatment which is valuable for predicting expected dimensions of phosphate groups utilizing Pauling's concept of bond strength without making ex-

Table 3. *Distances* (Å) *and angles* (°) *of the pyrophosphate group*

(*a*) Dimensions *observed* for phosphate tetrahedra; oxygen atoms have the same order with respect to coordination as used in (*b*). $\Delta 1 \times 10^{-3} = (i\text{–}j)_{obs} - (i\text{–}j)_{pre}$, $\Delta 2 = (\angle ijk)_{obs} - (\angle ijk)_{pre}$, $\Delta 3 \times 10^{-3} = (i\text{–}k)_{obs} - (i\text{–}k)_{cal}$.

i *j* *k*	*i*–*k*	Δ3	*ijk*	Δ2	*i*–*j*	Δ1
O(1)–P(1)–O(2)	2·553	46	110·7	2·7	1·610	−4
O(2)–P(1)–O(3)	2·548	−15	118·2	−2·7	1·493	9
O(3)–P(1)–O(4)	2·465	−53	106·7	−3·7	1·477	15
O(4)–P(1)–O(1)	2·424	−40	98·3	−1·8	1·593	−10
O(1)–P(1)–O(3)	2·515	0	109·0	−0·6		
O(2)–P(1)–O(4)	2·559	46	111·9	3·0		
O(7)–P(2)–O(5)	2·524	17	110·0	2·0	1·601	−13
O(5)–P(2)–O(6)	2·573	10	121·3	0·4	1·478	−6
O(6)–P(2)–O(4)	2·544	26	111·1	0·7	1·473	11
O(4)–P(2)–O(7)	2·486	22	101·4	1·3	1·611	8
O(7)–P(2)–O(6)	2·457	−58	106·0	−3·6		
O(5)–P(2)–O(4)	2·455	−58	105·2	−3·7		
P(1)–O(4)–P(2)	2·952 (2)		134·2			

(*b*) Dimensions predicted by Baur (1974); notations in parentheses indicate the coordination of the oxygen atoms

O(C)—P–O(2H)	2·507	108·0	1·614
O(2H)–P–O(1H)	2·563	120·9	1·484
O(1H)–P–O(P)	2·518	110·4	1·462
O(P)—P–O(C)	2·464	100·1	1·603
O(C)—P–O(1H)	2·515	109·6	
O(2H)–P–O(P)	2·513	108·9	

* The table of structure factors has been deposited with the British Library Lending Division as Supplementary Publication No. SUP 30644 (22 pp.). Copies may be obtained through The Executive Secretary, International Union of Crystallography, 13 White Friars, Chester CH1 1NZ, England.

plicit use of π-bonding or Coulombic repulsions in describing the phosphate pseudotetrahedron. His approach will be followed in this discussion.

The two phosphate moieties of DNPP, PO1, containing P(1), and PO2, containing P(2), are *conformationally* distinct. However, they are *configurationally* identical, so that they are equivalent in Baur's treatment. Their observed dimensions and the dimensions predicted by Baur are given in Table 3.

The parameters in the three parts of the table are ordered identically with respect to oxygen configuration. The discrepancies between observed and predicted parameters are given following each *observation*. The average of the individual discrepancies in P–O bond lengths ($\Delta 1$) is 0·010 Å, in O–P–O valence angles ($\Delta 2$) 2·2° and in O–O interactions ($\Delta 3$) 0·032 Å. For his entire data base Baur found these average discrepancies to be respectively, 0·010 Å, 1·5° and 0·020 Å. The agreement for the P–O bond lengths is entirely satisfactory. The discrepancies for some O–P–O valence angles (and O···O interactions) are larger than expected, indicating that some factor not correlated with Baur's parameters is distorting the pseudotetrahedra. For example, distortion due to shared polyhedra has been discussed by Baur (1972) for metallic salts of phosphates. Analysis of this structure indicates that non-bonded interactions between the phosphate oxygens and substituent atoms may cause distortions which can be predicted with a knowledge of the conformation. We propose that the O–P–O valence angles of a substituted oxygen will be decreased with respect to oxygens *anti* to the substituent and increased with respect to oxygens *syn* to the substituent; for di- and tri-substituted phosphates the distortions may reinforce or cancel one another. The conformation of the phosphates in DNPP, as shown in Fig. 4 (*b,c,e,f*), indicates that the angles O(3)–P(1)–O(4), O(4)–P(1)–O(1), O(7)–P(2)–O(6) and O(5)–P(2)–O(4) will be decreased relative to Baur's prediction. The expected general increase is observed among the other angles, except for an unexplained decrease in angle O(2)–P(1)–O(3).

Pyrophosphate conformation

The conformation of the pyrophosphate group is described in Fig. 4(*a–f*). The staggering around the P–O bonds in DNPP is not ideal, but the only exceptional interaction is the eclipsed conformation of P(1)–O(4)–P(2)–O(6). This is the smallest torsion angle observed among the phosphate esters and anhydrides so far studied. Of special interest are the torsion angles with respect to bridging oxygens (shown circled in Fig. 4). The succession of conformation found along P–O (bridging) bonds is alternately *syn* and *anti*, as defined by the conventions of Klyne & Prelog (1960).

In compounds with a divalent bridge between tetrahedrally bonded atoms (*e.g.* diphosphate anion) or a tetrahedrally bonded atom with two or more divalent bridges (*e.g.* naphthyl pyrophosphate), 1,3 interactions are important and must be considered in understanding the structure. Sundaralingam (1969) has noted the importance of the interaction of lone-pair electrons of the bridging oxygens to conformation. Pletcher & Sax (1966, 1972) have noted the tendency of the oxygens of phosphate moieties of di- and polyphosphates

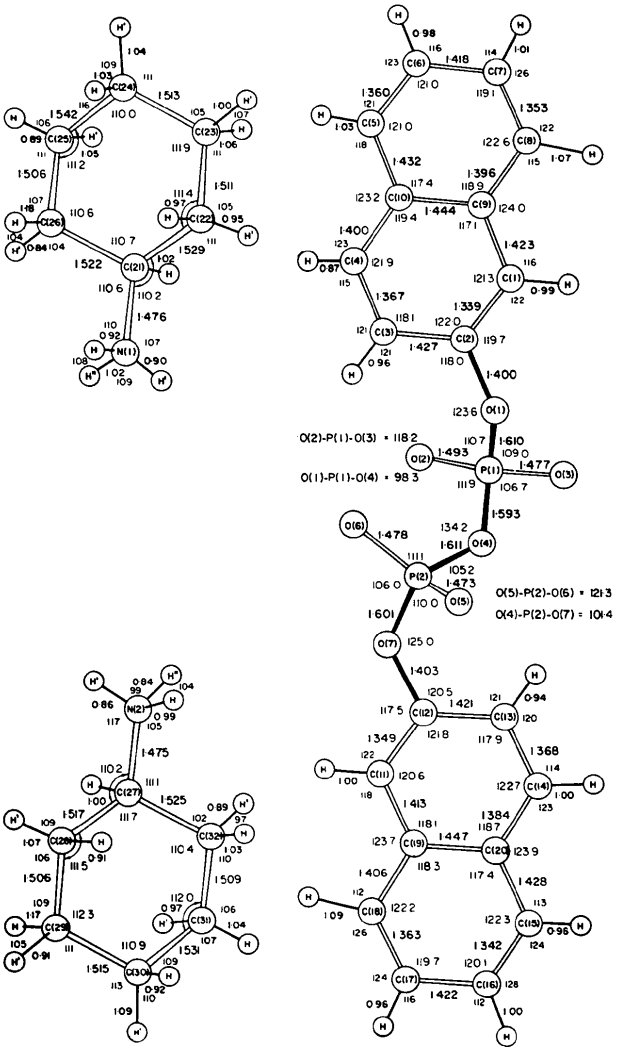

C(21)	- N(1)	- H''(N1)	110	C(24)	- C(25)	- H'(C25)	109	C(29)	- C(28)	- H (C28)	110
H(N1)	- N(1)	- H'(N1)	113	C(26)	- C(25)	- H'(C25)	112	H(C28)	- C(28)	- H'(C28)	119
N(1)	- C(21)	- H (C21)	109	H(C25)	- C(25)	- H'(C25)	107	C(28)	- C(29)	- H'(C29)	110
C(22)	- C(21)	- H (C21)	108	C(21)	- C(26)	- H (C26)	111	C(30)	- C(29)	- H (C29)	110
C(26)	- C(21)	- H (C21)	109	C(25)	- C(26)	- H'(C26)	119	C(29)	- C(30)	- H (C30)	104
C(21)	- C(22)	- H (C22)	105	C(27)	- N(2)	- H''(N2)	122	C(31)	- C(30)	- H'(C30)	110
C(23)	- C(22)	- H (C22)	106	H(N2)	- N(2)	- H'(N2)	108	C(30)	- C(31)	- H'(C31)	108
H(C22)	- C(22)	- H'(C22)	119	N(2)	- C(27)	- H (C27)	101	C(32)	- C(31)	- H'(C31)	104
C(22)	- C(23)	- H'(C23)	114	C(28)	- C(27)	- H (C27)	111	H(C31)	- C(31)	- H'(C31)	120
C(24)	- C(23)	- H (C23)	106	C(32)	- C(27)	- H (C27)	112	C(27)	- C(32)	- H (C32)	112
C(23)	- C(24)	- H (C24)	99	C(27)	- C(28)	- H (C28)	102	C(31)	- C(32)	- H'(C32)	125
C(25)	- C(24)	- H'(C24)	111								

Fig. 2. A schematic representation of the molecule showing the atomic numbering scheme and the final bond distances (Å) and angles (°). Estimated standard deviations are as follows: P–O = 0·004, C–O = 0·006, C–N = 0·007, C–C = 0·009, C–H = 0·07, N–H = 0·07 Å; P–P–O = 0·2, C–O–P = 0·3, O–C–C = 0·4, C–C–N = 0·5, C–C–C = 0·6, C–C–H = 4, C–N–H = 4, H–C–H = 5, H–N–H = 7°.

to have the staggered conformation when viewed along the P–P vector as shown in Fig. 5. These 1,3 interactions are conveniently visualized by means of the pseudo-torsion angles viewed along O···O and P···P vectors, respectively. The conformations shown in Fig. 4 (*g*,*h*,*i*) serve to demonstrate how critical these interactions may be (even in a structure where the staggering with respect to P–O vectors is far from ideal). The pseudo-torsion angles are not independent parameters but depend upon the bridge valence angle and the torsion angles along its bonds. Hence, the constraints imposed by the 1,3 interactions influence the torsion angles and *vice versa*. It is important to note that, in contrast to the 1,2 interactions where the bond directions are divergent, the 1,3 interactions *anti* to the bridge position involve nearly parallel or actually convergent bond (or lone-pair) directions. Recent *ab initio* calculations (Newton, 1973) on a phosphate diester give qualitative confirmation of some of the conformational constraints considered above.

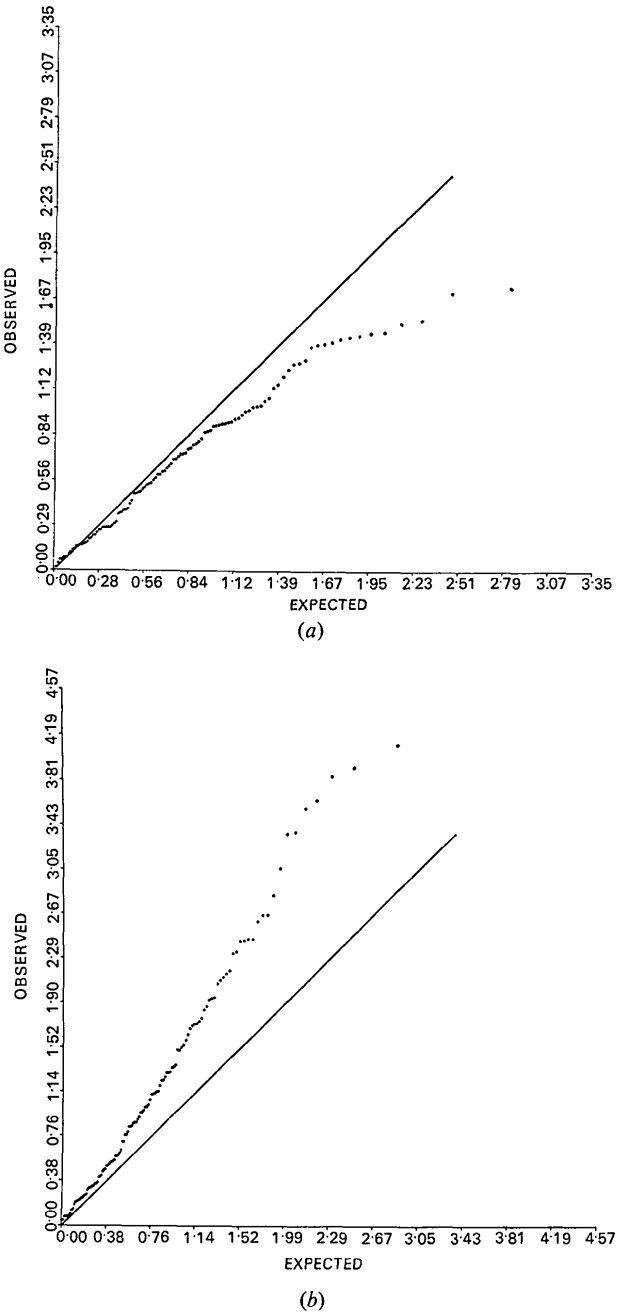

Fig. 3. Half-normal probability plots for the parameter differences $|\Delta p_i/\sigma(p_i)|$, comparing (*a*) bond distances and angles and (*b*) thermal parameters of atoms that are related by the pseudocenter of symmetry. The line with unit slope has been drawn.

Naphthyl groups

The average bond length of each naphthyl group is 1·396 Å, in good agreement with other determinations of naphthalene. The substitution causes alterations in individual bond lengths around the rings which we have not attempted to analyze. In addition, some warping of the naphthyl groups is apparent in the least-squares planes given in Table 4.

Table 4. *Planarity of the molecule*

(*a*) Deviations (Å × 10³) from the planes. Deviations for atoms defining the planes are marked with asterisks.

	NP1	NP2		NP1	NP2
C(1)	−4*	13	P(2)	−707	925
C(2)	29*	12	O(5)	−1902	2157
C(3)	0*	0	O(6)	−824	972
C(4)	−19*	−52	O(7)	154	110
C(5)	6*	−186	C(11)	384	−14*
C(6)	10*	−221	C(12)	280	57*
C(7)	11*	−181	C(13)	374	−1*
C(8)	−21*	−79	C(14)	461	−17*
C(9)	−7*	−58	C(15)	551	4*
C(10)	−3*	−102	C(16)	560	31*
O(1)	−44	156	C(17)	538	16*
O(2)	1974	−1851	C(18)	502	−20*
O(3)	1839	−1643	C(19)	472	−28*
P(1)	1149	−988	C(20)	508	−27*
O(4)	262	−44			

(*b*) The equations for the planes, expressed as direction cosines with respect to the crystallographic axes, are as follows:

NP1 $-0{\cdot}2689X+0{\cdot}2848Y-0{\cdot}9201Z=0{\cdot}004$ Å
NP2 $0{\cdot}2337X-0{\cdot}2516Y+0{\cdot}8086Z=0{\cdot}318$ Å

The angle between planes is 3·0°.

The ester oxygens deviate from the naphthyl planes to which they are bonded. O(1) is 0·044 Å from the plane of naphthyl group NP1, and O(7) is 0·110 Å from the plane of naphthyl group NP2. Considering the dianion as a whole, both naphthyl groups and the anhydride oxygen are coplanar with an estimated standard deviation of 0·06 Å.

Cyclohexylammonium ions

The average endocyclic bond length and valency angle found for the cyclohexylammonium ion containing

N(11), CA1, are, respectively, 1·520 (4) Å and 111·0 (3)°; for the other, CA2, we find, respectively, 1·517 (4) Å and 111·5 (2)°. Rao & Sundaralingam (1969) reported, respectively, 1·515 (4) Å and 111·4 (2)°. There is excellent agreement among these average parameters for the three determinations.

The individual parameters for CA1 and CA2 do not differ from the average values by more than two standard deviations. The average bond length is 1·519 Å, significantly shorter than the accepted value of 1·544 Å for sp^3–sp^3 single bonds. Application of the **TLS** tensors using the method of Schomaker & Trueblood (1968) to the refined thermal parameters (see below) results in a correction of the average bond length to 1·531 Å.

The rings, CA1, CA2 and CAR (Rao & Sundaralingam, 1969) have the expected chair conformation with the amine group taking an equatorial position. The torsion angles are shown in Fig. 6. The average endocyclic torsion angle for CA1, CA2 and CAR are, respectively, 56·1 (4)°, 54·7 (3)° and 54·9 (not given)°. Substituted chair cyclohexane rings may differ from $\bar{3}$ symmetry, where the torsion angles are all equivalent, to assume approximate 2 or m symmetry. Rohrer & Duax (1974) have proposed the use of root-mean-square (r.m.s.) discrepancies as indices for quantifying prominent conformational symmetry. If we consider the r.m.s. discrepancy of the torsion angles from $\bar{3}$ symmetry, we find for CA1, CA2 and CAR, respectively, 1·3°, 1·1° and 2·1° where the r.m.s. $\sigma = 0{\cdot}8$ for each ring. Only CAR shows a significant deviation from $\bar{3}$, having prominent m symmetry. The deviation from $\bar{3}$ symmetry is evidently not due to intramolecular forces.

Hydrogen bonding and packing

Each pyrophosphate moiety is hydrogen bonded to six different amines as shown in Fig. 7. The parameters of these hydrogen bonds are given in Table 5. There is a single hydrogen bond to each of the phosphoryl oxygens, O(3) and O(6), and two hydrogen bonds to each of the oxygens, O(2) and O(5). An interesting feature of the hydrogen bonding is the coplanarity of the atoms P(1^{iii}), O(2^{iii}), N(1^{i}) and N(2^{ii}) and of the atoms P(2^{v}), O(5^{v}), N(1^{i}) and N(2^{ii}). These two planes have e.s.d.'s of 0·009 and 0·005 Å, respectively; the angle between them is 2·5°. The hydrogen atoms of the bonds are significantly out of plane.

The principal intermolecular non-bonded interactions are between the interleaved naphthyl and cyclohexyl moieties, as may be seen in Fig. 7.

Rigid-body motion

Each cyclohexylammonium ion, naphthyl and phosphate group was treated as though it were a separate rigid body by utilizing the **TLS** tensors described by Schomaker & Trueblood (1968). The values of **T** and **L**, the position of the origin which symmetrizes **S** and the r.m.s. ΔU^{ij} are given in Table 6. In interpreting

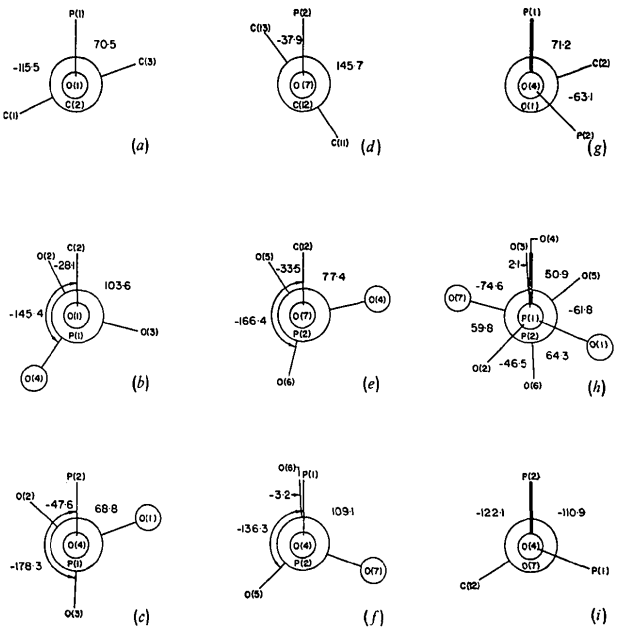

Fig. 4. Torsion angles (°) about the O–P and O–C bonds and projected angles about the P···P vector and the O···O vectors of adjacent bridging oxygen atoms. Bridging oxygen atoms are shown circled, and eclipsing bonds are bold. The average estimated standard deviation is 0·4°.

Table 5. *Hydrogen-bond lengths* (Å) *and angles* (°); *standard deviations are given in parentheses*

a	b	c	d	a–c	a–b	b–c	abc	bac	acd
N(1^{i})	-H(N1^{i})····	O(2^{iii})-	P(1^{iii})	2·844 (6)	0·92 (5)	1·94 (5)	166 (4)	10 (3)	127·8 (2)
N(1^{i})	-H′(N1^{i})····	O(3^{iv})-	P(1^{iv})	2·758 (6)	0·90 (7)	1·86 (7)	176 (7)	3 (5)	135·9 (2)
N(1^{i})	-H″(N1^{i})···	O(5^{v}) -	P(2^{v})	2·907 (6)	1·03 (11)	1·90 (11)	166 (9)	9 (6)	116·3 (2)
N(2^{ii})-	H(N2^{ii})····	O(5^{v}) -	P(2^{v})	2·900 (6)	0·99 (5)	1·94 (5)	163 (5)	11 (3)	155·6 (2)
N(2^{ii})-	H′(N2^{ii})···	O(6^{vi})-	P(2^{vi})	2·820 (6)	0·86 (6)	1·99 (6)	162 (6)	13 (4)	127·0 (2)
N(2^{ii})-	H″(N2^{ii})···	O(2^{iii})-	P(1^{iii})	2·806 (6)	0·84 (9)	1·99 (9)	163 (9)	12 (6)	141·0 (2)
N(1^{i})		O(2^{iii})	N(2^{ii})						91·2 (2)
N(1^{i})		O(5^{v})	N(2^{ii})						88·1 (2)

Symmetry code:

i	$1-x$,	$0{\cdot}5+y$,	$0{\cdot}5-z$
ii	$1-x$,	$-0{\cdot}5+y$,	$0{\cdot}5-z$
iii	$1-x$,	$1-y$,	$-z$
iv	$1+x$,	y,	z
v	$1-x$,	$1-y$,	$1-z$
vi	x,	y,	$-1+z$

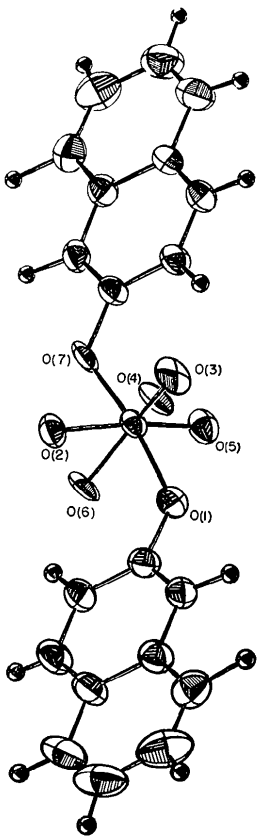

Fig. 5. A projection of the dinaphthyl pyrophosphate dianion down the P(1)···P(2) vector as drawn by the *ORTEP* program (Johnson, 1965) with thermal ellipsoids of the nonhydrogen atoms at the 50% probability level. The hydrogen atoms are represented by spheres having a fixed arbitary radius.

the rigid-body parameters their agreement with the observed values must be assessed. Half-normal probability plot analysis was used to compare the experimentally derived U^{ij}'s and their σ's to the U^{ij}'s calculated from rigid-body parameters for each moiety; the rigid-body model was assumed to have no error. The slopes, $S(\delta U)$, for least-squares lines through the points having a $\Delta U^{ij}/\sigma U^{ij}_{1s} \leq 2$ $\{\Delta U^{ij} = |U^{ij}(\text{exp.}) - U^{ij}(\text{rigid body})|\}$ are given in Table 6; also given are the maximum values for $\Delta U^{ij}/\sigma U^{ij}_{1s}$. It is concluded that the cyclohexylammonium ions and the naphthyl groups behave as rigid bodies within the error of the experiment. The bond distance corrections for the bonds in the naphthyl groups are almost uniform and average 0·004 Å, or about 0·5 e.s.d. For the cyclohexylammonium ions the corrections required vary from 0·007 to 0·019 Å, averaging 0·012 Å, or about 1·3 e.s.d.

The center of libration for each cyclohexylammonium ion lies near the N-substituted carbon, and the major axis of libration is nearly parallel to the C–N bond. This is as expected since the nitrogen atoms are held by hydrogen bonds, and the lowest moments of inertia are parallel to the average plane of the ring. Likewise, for each naphthyl group the center of libration lies near the esterified carbon. The axes of libration do not have readily interpretable directions.

It appears that the dominant motion of each phosphate is as a unit. While each of the oxygen atoms has additional covalent or hydrogen bonds, the geometry of these bonds is not as constraining as that of the phosphate pseudotetrahedron (consider the limited range of O···O distances in phosphate and the effectiveness of Baur's treatment). The r.m.s. deviations for the U^{ij}'s are reassuringly low; however, the probability plot analysis shows that the error in the rigid-body fit

Table 6. *Rigid-body motion parameters of the six segments of the structure*

(*a*) **T**, r.m.s. ΔU^{ij} and r.m.s. σU^{ij}_{1s} are given in Å × 10³. **L** is given in deg². The positions of the centers of libration are given in fractional coordinates.

	CA1	CA2	NP1	NP2	PO1	PO2
T_{11}	30 (2)	22 (2)	31 (2)	28 (1)	14 (2)	12 (2)
T_{22}	62 (2)	53 (1)	46 (2)	31 (1)	37 (2)	40 (2)
T_{33}	37 (4)	33 (4)	40 (3)	41 (2)	28 (2)	30 (2)
T_{12}	5 (1)	2 (1)	7 (1)	0 (1)	−2 (2)	0 (2)
T_{13}	−2 (2)	−2 (2)	1 (2)	−1 (1)	−2 (2)	2 (2)
T_{23}	−8 (2)	−8 (2)	1 (2)	4 (1)	0 (2)	−5 (2)
L_{11}	12 (3)	12 (3)	8 (2)	8 (1)	39 (8)	41 (7)
L_{22}	62 (8)	46 (7)	6 (6)	7 (4)	19 (8)	13 (4)
L_{33}	17 (2)	16 (2)	12 (2)	11 (1)	25 (10)	13 (5)
L_{12}	−24 (3)	2 (3)	−4 (2)	−2 (1)	−10 (10)	−2 (9)
L_{13}	4 (2)	6 (2)	4 (2)	1 (1)	−16 (6)	−10 (8)
L_{23}	5 (4)	4 (4)	−3 (3)	0 (2)	3 (5)	−8 (9)
x	0·1454	0·4144	0·2303	0·2053	0·1946	0·2619
y	0·0451	0·9281	0·3813	0·6324	0·4771	0·5320
z	0·3768	0·6929	0·2405	0·7110	0·3803	0·6293
r.m.s.ΔU^{ij}	2·6	2·5	3·3	2·0	1·6	1·4
r.m.s.σU^{ij}_{1s}	3·7	3·1	3·1	2·8	1·6	1·6

(*b*) Maximum value of $|U^{ij}(\text{exp.}) - U^{ij}(\text{rigid body})|/\sigma U^{ij}_{1s}$ and slope of the half normal probability plot of δU

$\Delta U^{ij}/\sigma U^{ij}_{1s}$	2·0	1·9	2·6	2·2	6·6	4·7
$S(\delta U)$	0·88	0·72	0·94	0·66	1·31	1·00

for PO1 is outside the expected error of the experiment. The corrections for the bond lengths are given in Table 7 and average 0·012 Å or 3·0 e.s.d. The center of libration for PO1 is 0·30 Å from P(1) in a direction away from O(3) and approximately in line with the P(1)–O(3) bond. For PO2 the center of libration is 0·69 Å from P(2) in a direction away from O(6) and approximately in line with the P(2)–O(6) bond. Internal modes of vibration evidently play a minor role in the phosphate motion, as these modes are perpendicular to the P–O bonds, and the center of libration is found to be considerably displaced from the P atom in each case.

Table 7. *Bond lengths* (Å) *within the pyrophosphate corrected for librational motion*

	Uncorrected	Corrected
P(1)–O(1)	1·610	1·625
P(1)–O(2)	1·493	1·503
P(1)–O(3)	1·477	1·490
P(1)–O(4)	1·593	1·607
P(2)–O(4)	1·611	1·623
P(2)–O(5)	1·478	1·488
P(2)–O(6)	1·473	1·479
P(2)–O(7)	1·601	1·613

As an additional test, structure factors were calculated using the β_{ij}'s calculated from the rigid-body parameters of all parts of the structure; the R value for the observed reflections increased from 0·064 to 0·069, a moderate but significant change.

The authors would like to thank Professor R. Shiono for providing programming assistance, Dr R. D. Rosenstein and Dr G. Blank for helpful discussions and Barbara Blackmond for technical assistance in preparing the *ORTEP* plots. We are especially grateful to Professor Werner Baur for making his work available to us prior to its publication. The computations were carried out in the University of Pittsburgh Computation Center. This research was partially supported by NIH Grant NS-09178.

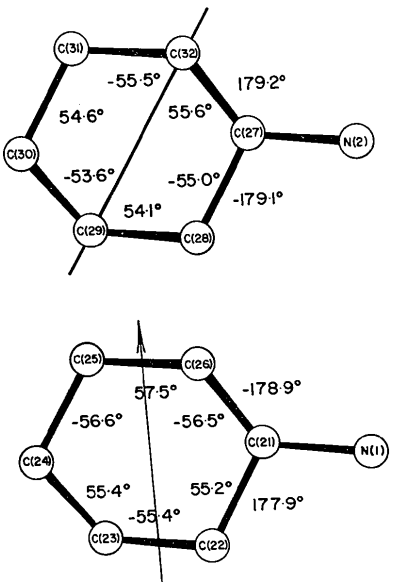

Fig. 6. Endo- and exocyclic torsion angles for the cyclohexylammonium ions. Prominent symmetry of the rings is indicated. The average estimated standard deviation is 0·7°.

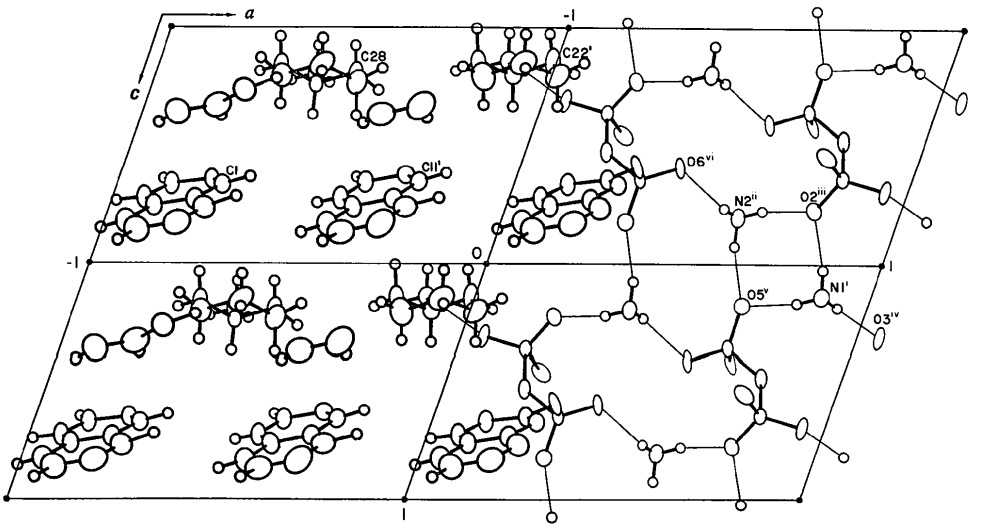

Fig. 7. A projection of the crystal structure down the *b* axis as drawn by the *ORTEP* program (Johnson, 1965) with thermal ellipsoids of the nonhydrogen atoms at the 50% probability level. The hydrogen atoms are represented by spheres having a fixed arbitrary radius. Two translations along the *a* and *c* axes are shown. In the *b* axial direction hydrocarbon atoms are restricted for clarity between 0·775 and 0·475 fractional translations on the left section and phosphate and amine atoms between 0·75 and 0·25 fractional translations on the right. Hydrocarbon packing and hydrogen bonding proceed parallel to the *ac* plane with weak interactions between hydrocarbon sheets in the *b* axial direction. Hydrogen bonding is depicted by thin lines.

References

ABRAHAMS, S. C. & KEVE, E. T. (1971). *Acta Cryst.* A**27**, 157–165.

ADAMS, M. J., MCPHERSON, A., ROSSMAN, M. G., SHEVITZ, R. W. & WANACOTT, A. J. (1970). *J. Mol. Biol.* **51**, 31–38.

BAUR, W. H. (1972). *Amer. Min.* **57**, 709–731.

BAUR, W. H. (1974). *Acta Cryst.* B**30**, 1195–1215.

CROMER, D. T. & WABER, J. T. (1965). *Acta Cryst.* **18**, 104–109.

CRUICKSHANK, D. W. J. (1970). In *Crystallographic Computing* edited by F. R. AHMED, S. R. HALL and C. P. HUBER, p. 195. Copenhagen: Munksgaard.

DUNITZ, J. D. & SEILER, P. (1972). *Acta Cryst.* B**29**, 589–595.

DUNNING, A. J. & VAND, V. (1969). *Acta Cryst.* A**25**, 489–491.

GERMAIN, G., MAIN, P. & WOOLFSON, M. M. (1971). *Acta Cryst.* A**27**, 368–376.

HAMILTON, W. C. & ABRAHAMS, S. C. (1972). *Acta Cryst.* A**28**, 215–218.

JOHNSON, C. K. (1965). *ORTEP.* Report ORNL-3794. Oak Ridge National Laboratory, Oak Ridge, Tennessee.

KLYNE, W. & PRELOG, V. (1960). *Experientia*, **16**, 521–523.

NEWTON, M. D. (1973). *J. Amer. Chem. Soc.* **95**, 256–258.

PICKER CORPORATION (1972). FACS-1 Disk Operating System. Cleveland, Ohio.

PLETCHER, J. & SAX, M. (1966). *Science*, **154**, 1331–1333.

PLETCHER, J. & SAX, M. (1972). *J. Amer. Chem. Soc.* **94**, 3998–4005.

RAE, A. D. (1973). *Acta Cryst.* A**29**, 74–77.

RAO, S. T. & SUNDARALINGAM, M. (1969). *Acta Cryst.* B**25**, 2509–2515.

ROHRER, D. C. & DUAX, W. L. (1974). *Acta Cryst.* Submitted for publication.

SCHOMAKER, V. & TRUEBLOOD, K. N. (1968). *Acta Cryst.* B**24**, 63–76.

SHIONO, R. (1971). *Crystallographic Computing Programs for IBM-7090 System.* Technical Report No. 48, Department of Crystallography, Univ. of Pittsburgh, Pittsburgh, Pa.

STEWART, R. F., DAVIDSON, E. R. & SIMPSON, W. T. (1965). *J. Chem. Phys.* **42**, 3175–3187.

SUNDARALINGAM, M. (1969). *Biopolymers*, **7**, 821–860.

Acta Cryst. (1975). B**31**, 85

trans-[Theophyllinatochlorobis(ethylenediamine)cobalt(III)] Chloride Dihydrate*

BY THOMAS J. KISTENMACHER

Department of Chemistry, The Johns Hopkins University, Baltimore, Maryland 21218, *U.S.A.*

(*Received* 9 *May* 1974; *accepted* 10 *July* 1974)

$[Co(C_2N_2H_8)_2Cl(C_7N_4O_2H_7)]Cl.2H_2O$ is triclinic, space group $P\bar{1}$, with $a=10{\cdot}034$ (3), $b=10{\cdot}711$ (4), $c=9{\cdot}499$ (4) A, $\alpha=109{\cdot}49$ (3), $\beta=93{\cdot}17$ (3), $\gamma=75{\cdot}87$ (2)°, $V=932{\cdot}8$ Å^3, $Z=2$, $D_m=1{\cdot}63$ (1), $D_c=1{\cdot}65$ g cm^{-3}. Intensities for 4315 independent reflections (4202 above zero) were collected by counter methods. The structure was solved by standard heavy-atom methods, and full-matrix least-squares refinement has led to final R values of 0·043 (excluding zeros) and 0·045 (including zeros). The final weighted R value and goodness-of-fit are 0·052 and 2·1, respectively. The coordination about the cobalt is approximately octahedral with the two bidentate ethylenediamine ligands in *trans* positions. The chloride ligand and N(7) of the theophylline moiety complete the coordination sphere. The complex exhibits interligand hydrogen bonds from the ethylenediamine ligands to the carbonyl group, C(6)–O(6), on theophylline.

Introduction

Crystals of $[Co(C_2N_2H_8)_2Cl(C_7N_4O_2H_7)]Cl$ were kindly supplied by Professor L. G. Marzilli and Mr C. H. Chang (1973, private communication). Preliminary photographs indicated a triclinic lattice. The unit-cell dimensions for the Friedel-reduced cell were derived from the 2θ, ω and χ values for 15 reflections. A density measurement, using flotation methods, suggested one formula unit and two waters of crystallization per asymmetric volume.

* This investigation was supported by the donors of the Petroleum Research Fund, administered by the American Chemical Society, and by a National Institutes of Health Biomedical Sciences Support Grant.

Intensity measurements were made on a Syntex $P\bar{1}$ computer-controlled diffractometer; the incident beam was monochromatized by a graphite crystal. The crystal used in data collection was a cut cube about 0·25 mm on an edge. Intensity data were collected with Mo $K\alpha$ radiation by the θ–2θ scan technique; individual scan speeds were determined by a rapid scan at the calculated Bragg peak, and the rate of scanning varied from 2 to 24° min^{-1}. Three standards were measured after every 100 reflections, and their intensities showed no unusual fluctuations or decay with time. A total of 4315 independent reflections in the $+h$ hemisphere to $2\theta=55°$ were surveyed; 4202 of these had intensities above zero and were assigned observational variances based on the equation: $\sigma^2(I)=S+(B_1+B_2)(T_S/2T_B)^2+$